RAPID COMMUNICATIONS

PHYSICAL REVIEW C

NUCLEAR PHYSICS

THIRD SERIES, VOLUME 51, NUMBER 5 MAY 1995

RAPID COMMUNICATIONS

The Rapid Communications section is intended for the accelerated publication of important new results. Manuscripts submitted to this section are given priority in handling in the editorial office and in production. A Rapid Communication in **Physical Review C** *may be no longer than five printed pages and must be accompanied by an abstract. Page proofs are sent to authors.*

η meson photoproduction on hydrogen near threshold

J. W. Price,*[1] G. Anton,[2] J. Arends,†[2] W. Beulertz,[2] A. Bock,[2] M. Breuer,[2] K. Büchler,[2] M. Clajus,[1] P. Detemple,‡[2] J. Hey,[2] D. Krämer,§[2] W. Meyer,[2] B. M. K. Nefkens,[1] G. Nöldeke,[2] W. Schneider,[2] and B. Zucht‖[2]

[1]*Department of Physics, University of California, Los Angeles, California 90024*

[2]*Physikalisches Institut der Universität Bonn, Nußallee 12, D-53115 Bonn, Germany*

(Received 19 December 1994)

The total cross section for $\gamma p \rightarrow \eta p$ near threshold has been measured using the PHOENICS tagging system at the ELSA electron facility of the Physikalisches Institut der Universität Bonn. The photons are created by bremsstrahlung, and are tagged by measuring the momentum of each electron after the photon has been emitted. The recoil proton from $\gamma p \rightarrow \eta p$ is detected by the AMADEUS counter setup in coincidence with the tagging system. Data were taken with AMADEUS at 3.3° in the laboratory, where the large Jacobian increases our event rate so that we obtain the cross section from threshold ($E_\gamma = 707.2$ MeV) to $E_\gamma \simeq 720$ MeV with adequate statistics. The $\gamma p \rightarrow \eta p$ events are identified by kinematics, dE/dx, and timing information. We find that in our energy region the production cross section is consistent with S-wave production.

PACS number(s): 13.60.Le, 14.40.Aq, 25.20.Lj, 14.20.−c

Photoproduction of η mesons on protons is a unique way to investigate the $N^*(I=1/2)$ resonances. There is considerable uncertainty about the strength of the ηN interaction. Arima *et al.* [1] quote the scattering length to be $a_{\eta N} = (0.98 + i0.37)$ fm; Wilkin [2] gives $a_{\eta N} = (0.55 \pm 0.2 + i0.3)$ fm; Bhalerao and Liu [3] quote $a_{\eta N} = (0.27 + i0.22)$ fm.

Near the threshold for η photoproduction are three resonances that can contribute as intermediate states: $P_{11}(1440)$, $D_{13}(1520)$, and $S_{11}(1535)$. We therefore expect resonance production to be important [4], in contrast to threshold production of the π^0; the nearest resonance to the $\pi^0 p$ threshold is the $P_{33}(1232)$, 150 MeV away.

At a photon energy of 730 MeV, the center-of-mass (c.m.) momentum of the outgoing η, $\tilde{p}_\eta$, is 100 MeV/c, or $\lambda\!\!\!^{-} \simeq 2$ fm. This wavelength is larger than the typical strong interaction length of $\simeq 1$ fm. Thus, up to this energy we expect the scattering to be predominantly S wave, with a flat angular distribution.

At threshold, both of the outgoing particles are at rest in the c.m. frame. This precludes production of the D_{13}; since it has $J = 3/2$, it cannot couple to the $|\eta N\rangle$ state with the orbital angular momentum $\ell = 0$. Production of the P_{11} is still possible, but the P_{11} lies well below the threshold for $\gamma p \rightarrow \eta p$; only the tail of this resonance would contribute. Since the S_{11} mass is near the threshold for η production, we expect $\gamma p \rightarrow \eta p$ in that energy range to be dominated by the S_{11}.

Studies of η photoproduction near threshold are important for the determination of the E_{0+} multipole strength. Quark models [5,6] favor a strong isovector excitation of the S_{11}; this is supported by the analysis of $\gamma p \rightarrow \pi N$ data by Bennhold and Tanabe [7]. On the other hand, Halderson and Rosenthal [8] in their analysis of the $\gamma d \rightarrow \eta d$ reaction favor an isoscalar excitation in order to account for the large cross section reported by Anderson and Prepost [9]. The structure

*Present address: Department of Physics, Rensselaer Polytechnic Institute, Troy, NY 12180–3590.

†Present address: Institut für Kernphysik, Universität Mainz, 55099 Mainz, Germany.

‡Present address: Institut für Mikrotechnik, Mainz, Germany.

§Present address: PPE-Division, CERN, CH-1211 Geneve 23, Switzerland.

‖Present address: MS Mikro Software, Bad Münstereifel, Germany.

 © 1995 The American Physical Society

of the ηNN vertex is not resolved between pseudovector and pseudoscalar coupling, and the strength of the coupling is only vaguely known.

A good theoretical understanding of η photoproduction has been hampered by a lack of data at threshold; there are only eight data points for the total cross section below $E_\gamma = 800$ MeV [10–12]. The paucity of data, combined with serious disagreements near threshold, have stimulated this measurement by our group; another measurement is being made at MAMI by the TAPS Collaboration [13]. Theoretical studies of $\gamma p \rightarrow \eta p$ are currently underway at RPI [4], Western Michigan University [14], and GWU-Mainz [15]. These studies would benefit from new data near threshold.

Our detection method is based on measuring only the recoil proton and inferring η production using two-body kinematics. For photon energies near threshold, the recoil protons have very little kinetic energy in the c.m. frame. Thus, they emerge in a small cone centered about the beam axis. As the energy decreases, the opening angle of this cone decreases until, at threshold, all the recoil protons emerge at 0°. Thus, a relatively small detector is adequate. The success of our method is based on the fact that close to threshold, the Jacobian becomes very large so that even a small cross section may be detectable above background. Detecting the proton alone does not allow one to distinguish background events in which the proton kinematics mimic that of η photoproduction. This can occur in the process $\gamma p \rightarrow \pi\pi p$, where the two pions have an invariant mass equal to that of the η. A proton from such a reaction constitutes a background that cannot be removed with cuts on the data. Such events are subtracted after all cuts have been applied.

The experiment was performed at ELSA, at the Physikalisches Institut der Universität Bonn, using the photon tagger in the PHOENICS area, described in detail in Ref. [16]. The tagger determined the energy and flux of the incident photon beam. The electron beam from ELSA is extracted onto a radiator, and photons are produced by bremsstrahlung. The electrons are momentum analyzed by a magnet, and are detected by a hodoscope of small scintillation tagging counters placed along the focal plane of the magnet.

The tagging counter that was hit determines the photon energy. The placement of the tagging counters corresponds to photon energy bins spaced approximately 5 MeV apart, and the energy distribution within each bin is roughly Gaussian, with a σ of 2.7 MeV. When quoting the photon energy, we use the variable $\langle E_\gamma \rangle^i$, which is the centroid of the energy range of the ith bin. The error in this quantity is typically less than 1 MeV. We define $\langle E_\gamma \rangle_{\gamma p \rightarrow \eta p}$ to be the actual mean photon energy for photons that have sufficient energy to produce ηs. This is only relevant for the bin at threshold, for which $\langle E_\gamma \rangle^i \neq \langle E_\gamma \rangle_{\gamma p \rightarrow \eta p}$ since the threshold lies within the bin.

The photon flux is determined by scalers connected to each of the tagging counters. This number is related to the number of photons that strike the target, but must be corrected for two effects. The first involves the probability that a count in the tagging system indeed corresponds to a photon in the target. This is measured during the experiment by placing a lead glass detector in coincidence with the tagging system, and measuring the ratio P^i_γ for each tagging counter, where

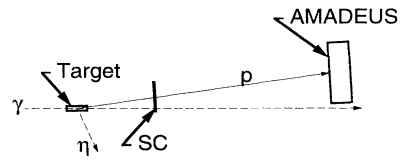

FIG. 1. The setup for the $\gamma p \rightarrow \eta p$ measurement. The figure is not shown to scale; the dimensions are given in the text.

$$P^i_\gamma \equiv N^i_{e\gamma} / N^i_e , \tag{1}$$

$N^i_{e\gamma}$ is the number of coincidences between a count in the ith tagging counter and the lead glass detector, and N^i_e is the number of single hits in the ith tagging counter. The second effect is that of accidentals in the tagging system. This is removed by looking only at events in which there was a single hit in the tagging system, and correcting the photon flux by the fraction of single hit events for each tagging counter. The combined effect of both of these corrections introduces an uncertainty of approximately 5% to the photon flux.

The detector setup for the experiment is shown in Fig. 1. The tagged photons interacted in a cylindrical liquid hydrogen target, 2 cm in diameter, and 8.0 ± 0.1 cm long. The axis of the target coincided with the photon beam. The recoil protons from $\gamma p \rightarrow \eta p$ were detected by a thin scintillation counter (SC) and the AMADEUS detector. SC consisted of a sheet of plastic scintillator viewed by photomultiplier tubes (PMTs) at both ends. AMADEUS, described in Ref. [17], consisted of a large block ($25 \times 40 \times 8$ cm^3) of plastic scintillator and a plexiglass light guide, viewed by 12 PMTs arranged in a rectangular array on the rear face of the light guide. It has excellent spatial and timing resolution, superior to a hodoscope with a similar number of PMTs. SC was placed 63 cm from the target, and AMADEUS was 286 cm from the target. Both detectors were at 3.3° in the laboratory. This angle was chosen to place AMADEUS as close as possible to the beam without placing it directly in the beam.

Timing and pulse height information were recorded for all PMTs. The two SC timing signals went into a mean timer to produce the start signal used for all TDCs. The mean timer reduced the dependence of the timing on the proton's impact position on the SC. The event trigger consisted of a triple coincidence between the tagging system, SC, and AMADEUS. At least two of the twelve PMTs in AMADEUS were required to fire, to reduce the background from low-energy electrons produced in the target. Several runs were taken with an empty target. These runs proved that the target walls gave a negligible contribution to the number of events, and were not used further in the analysis.

The main steps of the analysis were (i) the selection of proton events, (ii) the determination of the photon energy associated with the event, (iii) subtracting the background due to multipion photoproduction (predominantly $\gamma p \rightarrow \pi\pi p$), and (iv) determining the number of $\gamma p \rightarrow \eta p$ events. Details of the analysis may be found in Ref. [18].

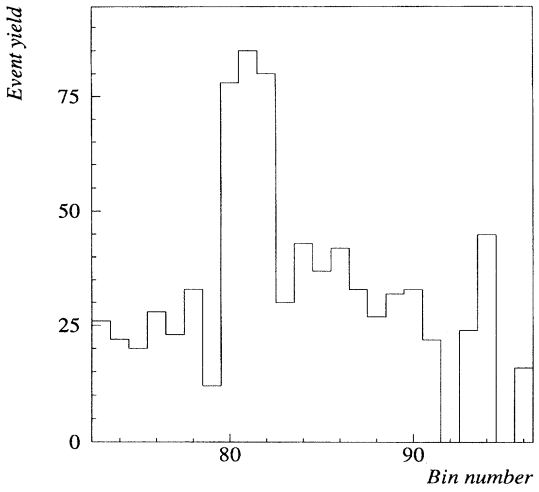

FIG. 2. The yield in each energy bin for proton events in AMADEUS. The η production threshold lies in bin 80. Each bin corresponds to approximately 5 MeV.

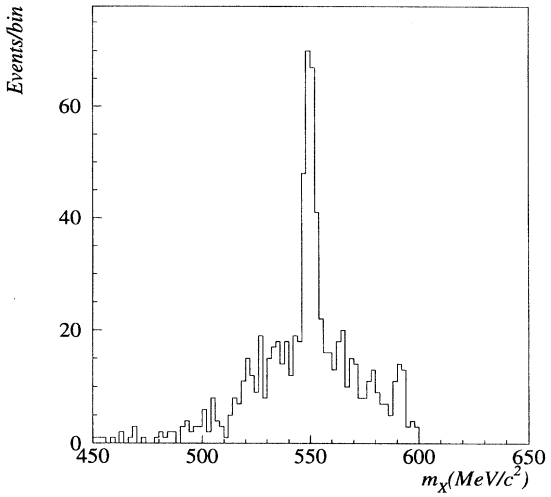

FIG. 3. The missing mass, m_X, for the process $\gamma p \rightarrow pX$ (675 MeV$<E_\gamma<$800 MeV).

The raw data contains mostly proton and electron events not removed by the hardware trigger. These can be separated very well by making use of the relationship between the pulse height in the SC (E_{SC}) and the time of flight between the SC and AMADEUS ($TOF_{SC\text{-}AM}$). Electrons, which all travel at c, show up as a vertical band in a scatter plot of $TOF_{SC\text{-}AM}$ vs E_{SC}. Proton events lie on a diagonal band. We project this scatter plot onto a diagonal line perpendicular to the proton band, and then place cuts around the resulting proton peak. We estimate the efficiency for proton detection by this method to be approximately 99%, and that less than 1% of the electrons remain after this cut.

The nominal calibration of the photon tagger [16] determines the relative energies of each bin to sufficient precision. Because the cross section rises very rapidly near threshold, it was necessary to determine $\langle E_\gamma \rangle$ for each energy bin relative to the η threshold as accurately as possible. The original calibration was used as a starting point. We then applied a simple additive shift to all the photon energies:

$$\langle E_\gamma \rangle^{i\prime} = \langle E_\gamma \rangle^i + \Delta E_\gamma, \tag{2}$$

where the values of $\langle E_\gamma \rangle^i$ were taken from the original calibration, and ΔE_γ was to be determined. The error resulting from this calibration is negligible compared to the overall calibration uncertainty. We used the data to determine ΔE_γ by two different methods, both based on the known threshold for η photoproduction, E_γ^{thr}.

The first method assumes an S-wave dependence for the cross section, and makes use of the sudden increase in the event yield as the photon energy crosses E_γ^{thr}. This is shown in Fig. 2. The background is due mainly to two and three pion production. After subtracting this background (estimated as the average yield below threshold) for each energy bin, we are left with the yield for $\gamma p \rightarrow \eta p$ for the ith bin, N_i. This obeys the proportionality relation

$$N_i \propto A_i(\langle E_\gamma \rangle) \langle \sigma_i(\langle E_\gamma \rangle) \rangle, \tag{3}$$

where $A_i(\langle E_\gamma \rangle)$ is the AMADEUS acceptance for the ith bin calculated by Monte Carlo, and $\langle \sigma_i(\langle E_\gamma \rangle) \rangle$ is the average cross section for $\gamma p \rightarrow \eta p$ for photons associated with the ith bin. By comparing the ratio of the yields for the first two bins above threshold obtained from the data with that expected from Eq. (3), we can determine $\langle E_\gamma \rangle$ for the bin at threshold. The difference between this energy and the energy obtained in the original calibration is ΔE_γ.

The second method utilizes the missing mass for the process $\gamma p \rightarrow pX$:

$$m_X = [2(m_p^2 + \langle E_\gamma \rangle m_p - \langle E_\gamma \rangle E_p + \langle E_\gamma \rangle p_p \cos\theta_p - E_p m_p)]^{1/2}, \tag{4}$$

where m_p is the proton mass (= 938.27 MeV/c^2), E_p is the total energy of the recoil proton, p_p ($=\sqrt{E_p^2 - m_p^2}$) is its momentum, and θ_p is its angle, all measured in the laboratory system. We calculate E_p and p_p at the $\gamma p \rightarrow pX$ vertex by measuring $TOF_{SC\text{-}AM}$. The energy thus obtained is corrected for energy loss between the target and AMADEUS. The peak in the m_X spectrum (see Fig. 3) was taken to correspond to the η, and ΔE_γ was determined by setting the scale such that this peak lies at m_η (= 547.45 MeV/c^2).

Both of these methods resulted in an uncertainty in $\langle E_\gamma \rangle$ of 0.6 MeV. The experiment was performed with three different settings of the tagging magnet, which entailed three separate calibrations.

After all the cuts have been made to remove the electron background, there was still significant background due to multipion production. The quantity $\delta p/p$ was defined as

$$\delta p/p \equiv (p_p - p_p^0)/p_p^0, \tag{5}$$

where p_p^0 is the proton laboratory momentum at the threshold for $\gamma p \rightarrow \eta p$ (= 447 MeV/c). Because the energies used in this experiment are well above the threshold for multipion production (for $\gamma p \rightarrow \pi\pi p$, E_γ^{thr} = 308.8 MeV; for $\gamma p \rightarrow \pi\pi\pi p$, E_γ^{thr} = 492.3 MeV), the contribution of the background to the $\delta p/p$ spectra is constant with photon en-

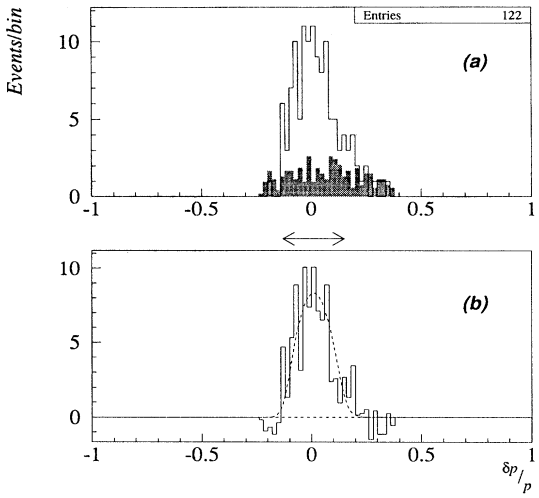

FIG. 4. (a) The raw spectrum of the momentum dispersion, $\delta p/p$, defined in Eq. (5), for $\langle E_\gamma \rangle_{\gamma p \to \eta p} = 710.1 \pm 0.9$ MeV. The shaded region is the background, normalized by the photon flux. "Entries" refers to the number of counts in the total spectrum. (b) The $\delta p/p$ spectrum for $\langle E_\gamma \rangle_{\gamma p \to \eta p} = 710.1 \pm 0.9$ MeV, after subtracting the background. The dashed curve is the expected spectrum from Monte Carlo. The arrows indicate the range used to determine the number of events. Note that the zero level on the Y axis has been shifted.

ergy to approximately 5%. We can therefore use the $\delta p/p$ spectra below threshold for $\gamma p \to \eta p$ to approximate the background. Figures 4(a) and 5(a) show examples of the background subtraction at two different energies. The two-peak structure in Fig. 5 is due to the limited acceptance of AMADEUS at higher E_γ. The peak at positive $\delta p/p$ corresponds to protons moving forward in the c.m. frame, and the negative $\delta p/p$ peak corresponds to protons moving backward in the c.m. frame.

After subtracting the background, the number of events was calculated by determining the allowed range for $\delta p/p$

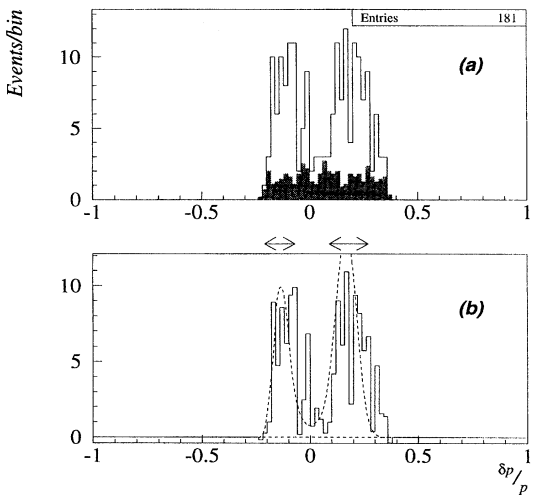

FIG. 5. (a) Same as Fig. 4(a) for $\langle E_\gamma \rangle = 718.7 \pm 0.7$ MeV. (b) Same as Fig. 4b for $\langle E_\gamma \rangle = 718.7 \pm 0.7$ MeV.

TABLE I. Total cross section σ for η production in the reaction $\gamma p \to \eta p$ as a function of the mean photon energy $\langle E_\gamma \rangle_{\gamma p \to \eta p}$.

$\langle E_\gamma \rangle_{\gamma p \to \eta p}$ (MeV)	$\sigma(\pm$ stat. $\pm$ syst.) (μb)
708.6	4.2 ± 1.6 ± 2.6
709.4	2.6 ± 0.5 ± 0.6
710.1	3.8 ± 0.6 ± 0.4
711.1	4.4 ± 0.6 ± 0.4
713.3	6.6 ± 0.7 ± 1.0
714.8	7.4 ± 1.1 ± 1.2
716.3	7.5 ± 1.3 ± 1.1
718.7	7.7 ± 1.1 ± 1.0

using Monte Carlo and adding up the histogram bins in that range. Examples of the event extraction are given in Figs. 4(b) and 5(b). The $\delta p/p$ range obtained from Monte Carlo is shown by the arrows above the figures.

The detector acceptance was determined by a Monte Carlo simulation using the GEANT code. The acceptance has a strong dependence on the energy near threshold, which contributes a systematic uncertainty of approximately 8% for $\langle E_\gamma \rangle^i > 708$ MeV ($\langle E_\gamma \rangle_{\gamma p \to \eta p} > 709.6$ MeV), and increasing linearly below that point, to approximately 30% at $\langle E_\gamma \rangle^i = 705$ MeV ($\langle E_\gamma \rangle_{\gamma p \to \eta p} = 708.7$ MeV). This was our dominant systematic uncertainty. Additional uncertainties result from the target thickness, the determination of the photon flux, and the background normalization.

The analysis efficiency was evaluated by applying the cuts used in the analysis to the simulated data. The resulting efficiency is approximately energy independent, with a value of 87±4.9 %.

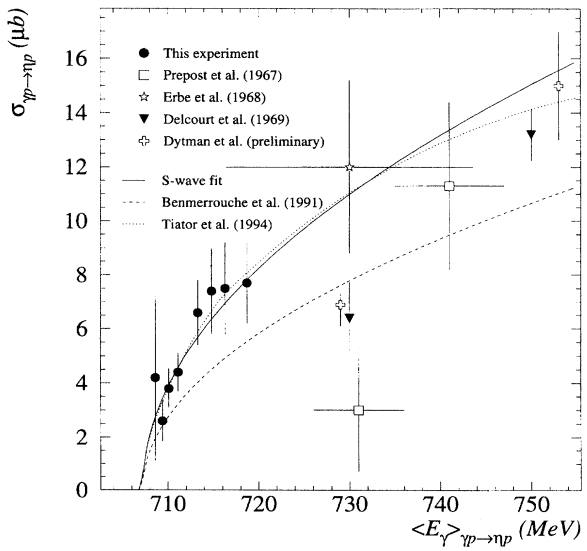

FIG. 6. Our results for the total cross section for $\gamma p \to \eta p$ are shown in solid circles. Prepost *et al.* data are from Ref. [10]; Delcourt *et al.*, Ref. [11]; Erbe *et al.*, Ref. [12]; Dytman *et al.*, from Ref. [19]. The solid line is the result of a fit of an S-wave production cross section to our points; the model of Benmerrouche *et al.* is from Ref. [4]; Tiator *et al.*, Ref. [15] for PS coupling and $g^2_{\eta NN}/4\pi = 0.5$.

The results of our experiment are given in Table I. Figure 6 shows our results, with the previous data shown for comparison. The statistical and systematic uncertainties have been added in quadrature. The solid line is the result of a fit to our points assuming an S-wave dependence with a constant matrix element for the cross section. Assuming the energy dependence of the cross section follows our S-wave fit, our results disagree with the preliminary results of Dytman *et al.* [19] at $\langle E_\gamma \rangle_{\gamma p \to \eta p} = 729$ MeV, but the agreement is much better at 753 MeV. The effective Lagrangian approach of Benmerrouche, Mukhopadhyay, and Zhang indicates some inconsistency of the present data with the older data base. The fact that the curve of Benmerrouche and Mukhopadhyay lies below our data is evidence of this. However, they claim that the results of this experiment are consistent with preliminary results from the Mainz experiment, with a value of $A_{1/2}$ in the vicinity of 0.1 $\mathrm{GeV}^{-1/2}$ [20]. The calculation of Tiator *et al.* agrees well with our data, using a pseudoscalar coupling constant of 0.5 [15].

The effect of the S_{11} on η photoproduction is clear: 5 MeV above threshold, the cross section for $\gamma p \to \eta p$ is an order of magnitude larger than that for $\gamma p \to \pi p$ at the corresponding energy above threshold. The proximity of the S_{11} to the $\gamma p \to \eta p$ threshold enhances the cross section greatly.

We have shown that our technique is a viable means of measuring η production near threshold. It is based solely on the detection of the recoil proton, and exploits the high acceptance and signal/background ratio available in the forward direction to compensate for the small cross section that has thus far prevented precision measurements. It is not as useful at photon energies far above threshold, due to the limited acceptance and lower signal/background ratio.

The authors wish to thank the ELSA staff for the quality of the beam. This research was supported in part by the Bundesministerium für Forschung und Technologie and the U.S. Department of Energy.

[1] M. Arima, K. Shimize, and K. Yazaki, Nucl. Phys. **A543**, 613 (1992).
[2] C. Wilkin, Phys. Rev. C **47**, R938 (1993).
[3] R. S. Bhalerao and L. C. Liu, Phys. Rev. Lett. **54**, 865 (1985).
[4] M. Benmerrouche and N. C. Mukhopadhyay, Phys. Rev. Lett. **67**, 1070 (1991).
[5] R. Koniuk and N. Isgur, Phys. Rev. D **21**, 1868 (1980).
[6] F. Foster and G. Hughes, Rep. Prog. Phys. **46**, 1445 (1983).
[7] C. Bennhold and H. Tanabe, Nucl. Phys. **A530**, 625 (1991).
[8] D. Halderson and A. S. Rosenthal, Nucl. Phys. **A501**, 856 (1989).
[9] R. L. Anderson and R. Prepost, Phys. Rev. Lett. **23**, 46 (1969).
[10] R. Prepost, D. Lundquist, and D. Quinn, Phys. Rev. Lett. **18**, 82 (1967).
[11] B. Delcourt, J. Lefrançois, J. P. Perez-Y-Jorba, and G. Sauvage, Phys. Lett. **29B**, 75 (1969).
[12] R. Erbe *et al.*, Phys. Rev. **175**, 1669 (1968).
[13] B. Krusche *et al.*, Phys. Rev. Lett. (to be published).
[14] A. S. Rosenthal, T. Forest, and M. Gonzales, Phys. Rev. C **44**, 2765 (1991).
[15] L. Tiator, C. Bennhold, and S. S. Kamalov, Nucl. Phys. **A580**, 455 (1994).
[16] P. Detemple *et al.*, Nucl. Instrum. Methods **A321**, 479 (1992).
[17] G. Anton, J. Arends, W. Beulertz, and J. Hey, Nucl. Instrum. Methods **A310**, 631 (1991).
[18] J. Price, Ph.D. thesis, UCLA, 1993.
[19] S. A. Dytman *et al.*, this issue, Phys. Rev. C **51**, 2710 (1995).
[20] N. C. Mukhopadhyay (private communication).